Conditionally filtered diffusion of mixture fraction and temperature in turbulent partially premixed flames

Jian Cai [a], Robert S. Barlow [b], Adonios N. Karpetis [c], Chenning Tong [a,*]

[a] *Department of Mechanical Engineering, Clemson University, Clemson, SC 29634-0921, USA*
[b] *Combustion Research Facility, Sandia National Laboratories, Livermore, CA 94551, USA*
[c] *Department of Aerospace Engineering, Texas A&M University, College Station, TX 77843, USA*

Available online 19 August 2010

Abstract

Recent studies have shown that the subgrid-scale (SGS) mixture fraction has different structures and probability distributions for different SGS scalar variances. We study the effects of these structures on the scalar diffusion and temperature diffusion in the context of large-eddy simulation (LES) of turbulent combustion. Line images obtained in turbulent partially premixed (Sandia) flames are used to analyze the scalar and temperature diffusion filtered conditionally on the scalar and temperature, which must be correctly modeled in LES. The results show that for small SGS variance the scalar and temperature diffusion have a relatively simple structure. For large SGS variance the diffusion is much more complex, with the flamelet structure and local extinction playing important roles. The results show that it is important that mixing models for filtered density function methods be able to account for the different SGS mixture fraction and temperature structures for small and large SGS variance.
© 2010 Published by Elsevier Inc. on behalf of The Combustion Institute.

Keywords: Turbulent flames; Large-eddy simulation; Filtered density function; Turbulent mixing

1. Introduction

Turbulent mixing and turbulence–chemistry interaction are key processes in turbulent combustion. Accurate predictions of turbulent flames depend critically on correct modeling of these processes. In large-eddy simulation (LES) of turbulent combustion mixing by the large, resolved scales is computed while the effects of the subgrid scales are modeled. Specifically, the subgrid-scale (SGS) scalar mixing and the resulting instantaneous distribution of scalar values in each grid volume, which is the species filtered joint mass density function (FMDF), must be faithfully represented in order to accurately predict the chemical reaction rate [1,2]. Modeling the FMDF, therefore, is the main challenge in LES and requires knowledge of SGS mixing and its interaction with chemistry.

Our recent studies [3–8] have shown that the SGS mixture fraction at a fixed location has qualitatively different filtered density function (FDF) shapes and structures depending on the *instantaneous* SGS scalar variance. When the SGS variance is small compared to its mean value, the distribution of the SGS scalar is close to Gaussian, indicating well mixed SGS scalar fields. When the SGS variance is large compared to its mean value, the distribution is bimodal, indicating highly non-premixed SGS scalar fields. In a

---
* Corresponding author. Fax: +1 864 6564435.
  E-mail address: ctong@ces.clemson.edu (C. Tong).

flame this mixing scenario would indicate that the fuel lean and rich regions of the SGS fields are highly segregated. There is a sharp interface separating the two regions, across which there is a large scalar value jump (can be as large as the integral-scale fluctuations). The conditional SGS structure on average resembles that of a counter-flow diffusion flame, which is a model for laminar flamelets.

The well-mixed and the highly non-premixed SGS mixture fraction fields have strong influences on the flame structure. The former is likely to result in distributed reaction zones while the latter supports laminar flamelets [8,9]. The mixture fraction–temperature filtered mass density function (FMDF) and the conditionally filtered dissipation rates of the mixture fraction and the temperature also are consistent with distributed reaction zones and laminar flamelets, respectively. Here we use the term "flamelets" to describe the thin physical flame structure rather than any modeling approach; therefore, we simply refer to them as flamelets hereafter. In this study we investigate the effects of the SGS mixture fraction structure on the conditional scalar diffusion and the temperature diffusion in turbulent partially premixed flames, which evolve the FMDF of mixture fraction and temperature:

$$
\begin{aligned}
F_{\xi TL}(\hat{\xi}, \widehat{T}; \mathbf{x}, t) &= \langle \rho(\mathbf{x}, t)\delta(\xi - \hat{\xi})\delta(T - \widehat{T}) \rangle_\ell \\
&= \int \rho(\mathbf{x}', t)\delta(\xi - \hat{\xi})\delta(T - \widehat{T}) \\
&\quad \times G(\mathbf{x} - \mathbf{x}')d\mathbf{x}',
\end{aligned}
\tag{1}
$$

where ξ, T, $\hat{\xi}$, and $\widehat{T}$ are the mixture fraction, temperature, and their sample-space variables, respectively. ρ is the fluid density. The subscripts ℓ and L denote conventional and Favre filtered variables, respectively. The knowledge of these diffusion terms is a first step in understanding the SGS turbulence–chemistry interaction and an important step toward understanding the SGS mixing of multiple reactive scalars.

2. Experimental data and processing procedures

We use experimental data obtained in piloted turbulent partially premixed methane with a 1:3 ratio of CH_4 to air by volume (Sandia flame D and E, see Refs. [10,11]). The measurements employed combined line-imaging of Raman scattering, Rayleigh scattering, and laser-induced CO fluorescence. Simultaneous measurements of major species (CO_2, O_2, CO, N_2, CH_4, H_2O, and H_2), mixture fraction (obtained from all major species), and temperature were made. The mixture fraction is calculated using a variation of Bilger's definition, which has been modified by excluding the oxygen terms. The length of the imaging line is 6.13 mm with a resolution of 0.2044 mm.

Measurements of the filtered density functions require spatial filtering of scalar fields. In this work one-dimensional filtering is employed. In LES filtering is generally performed in three dimensions. Our previous results [5] have shown, however, that the FDF obtained with a one-dimensional filter is qualitatively the same as those with a two-dimensional filter, which has been shown to be a very good approximation of three-dimensional filters, with errors of approximately 5% for the rms resolvable- and subgrid-scale variables [12]. For similar bimodality the corresponding SGS variance is somewhat larger for a one-dimensional filter. For conditional diffusion (and dissipation), the primary effect of a one-dimensional filter is a somewhat higher SGS variance. But the increase is much smaller than the change needed to affect the shape of the conditional diffusion. Consequently, one-dimensional filters are expected to yield similar results. To ensure that the results are relevant to LES the filter sizes Δ employed in this work (3.0 and 4.9 mm) are significantly larger than the dissipative (Corrsin) scales (0.065–0.106 mm [13]), such that the subgrid scales contain sufficient fluctuations to interact with chemistry, allowing the physics of the SGS mixing and its interaction with chemistry to be related to inertial-range dynamics. Previous studies (e.g., Refs. [3,5]) have shown that when the filter size is much larger than the dissipation scales the properly scaled conditional statistics are not sensitive to the filter size.

3. Results

The scalar diffusion and temperature diffusion are analyzed using their conditional samples. We use the Favre filtered mixture fraction, $\langle \xi \rangle_L = \langle \rho\xi \rangle_\ell / \langle \rho \rangle_\ell$, and the Favre SGS scalar variance,

$$
\begin{aligned}
\langle \xi''^2 \rangle_L &\equiv \frac{1}{\langle \rho \rangle_\ell} \int F_{\xi L}(\hat{\xi}; \mathbf{x}, t)(\xi - \langle \xi \rangle_L)^2 d\xi \\
&= \langle \rho\xi^2 \rangle_\ell / \langle \rho \rangle_\ell - \langle \xi \rangle_L^2,
\end{aligned}
\tag{2}
$$

as conditioning variables.

The scalar and temperature diffusion filtered conditionally on both the mixture fraction and temperature, $\langle \langle \frac{1}{\rho} \frac{\partial}{\partial y}(\rho D \frac{\partial \xi}{\partial y})|\xi, T \rangle_\ell | \langle \xi \rangle_L, \langle \xi''^2 \rangle_L \rangle$ and $\langle \langle \frac{1}{\rho} \frac{\partial}{\partial y}(\rho D_T \frac{\partial T}{\partial y})|\xi, T \rangle_\ell | \langle \xi \rangle_L, \langle \xi''^2 \rangle_L \rangle$ are shown in Figs. 1–5. In the FMDF equation these variables appear in the terms transporting the FMDF in the ξ and T spaces, respectively; therefore, they are the two components of the diffusion velocity of the FMDF in the $\xi - T$ space. In the present study we use streamlines and isocontours to represent the direction and the magnitude of the diffusion velocity, respectively. The diffusion terms are calculated using 10th-order central differencing. The mixture fraction diffusion and the temperature
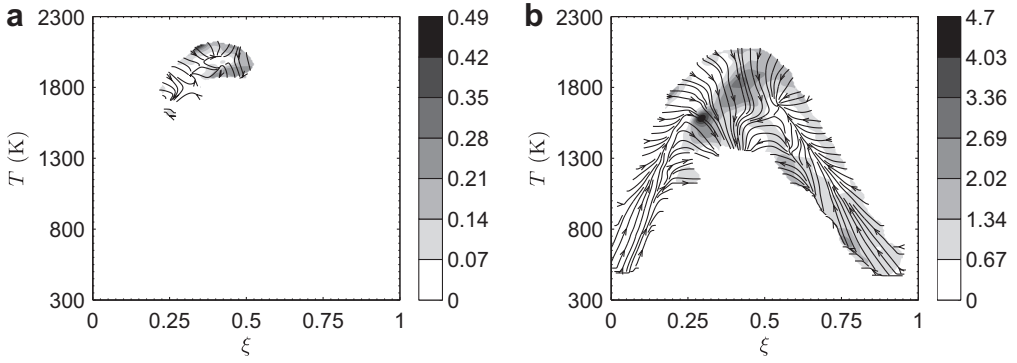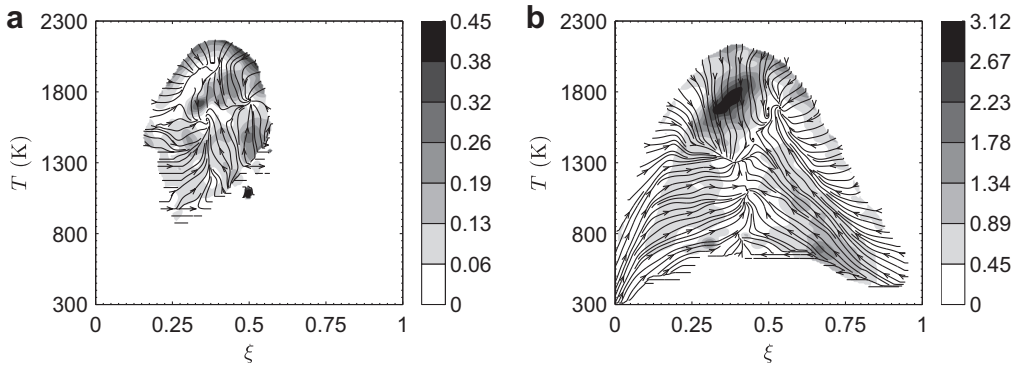
Fig. 1. The scalar diffusion and temperature diffusion filtered conditionally on both the mixture fraction and temperature for $\Delta = 3.0$ mm and $\langle \xi \rangle_L = \xi_s$ at $x/D = 7.5$ in flame D. The two diffusion terms are given as streamlines with the magnitude of the diffusion velocity in the $\xi - T$ space in grayscales. (a) $\langle \xi''^2 \rangle_L = 0.0013$; (b) $\langle \xi''^2 \rangle_L = 0.066$.

Fig. 2. The scalar diffusion and temperature diffusion filtered conditionally on both the mixture fraction and temperature for $\Delta = 3.0$ mm and $\langle \xi \rangle_L = \xi_s$ at $x/D = 15$ in flame D. (a) $\langle \xi''^2 \rangle_L = 0.003$ and (b) $\langle \xi''^2 \rangle_L = 0.069$.
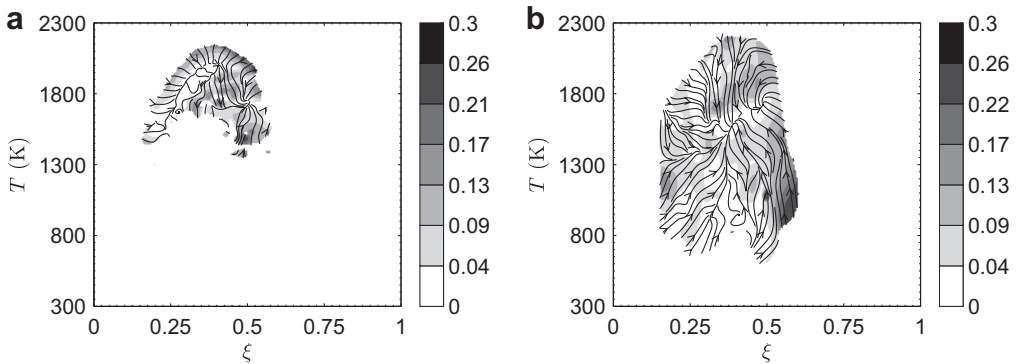

Fig. 3. The scalar diffusion and temperature diffusion filtered conditionally on both the mixture fraction and temperature for $\langle \xi''^2 \rangle_L = 0.003$ and $\langle \xi \rangle_L = \xi_s$ at $x/D = 15$ in flame D. $\Delta = 3.0$ mm. (a) $\langle T \rangle_L > 1800$ K and (b) $\langle T \rangle < 1800$ K.

diffusion are normalized by the filtered scalar dissipation rate, the SGS variance, and the maximum values of the mixture fraction (1.0) and temperature (2300 K), respectively.

The results for flame D at $x/D = 7.5$ is shown in Fig. 1. For small SGS variance, the streamlines appear to move first towards a manifold close to the ridgeline of the FMDF, in the direction
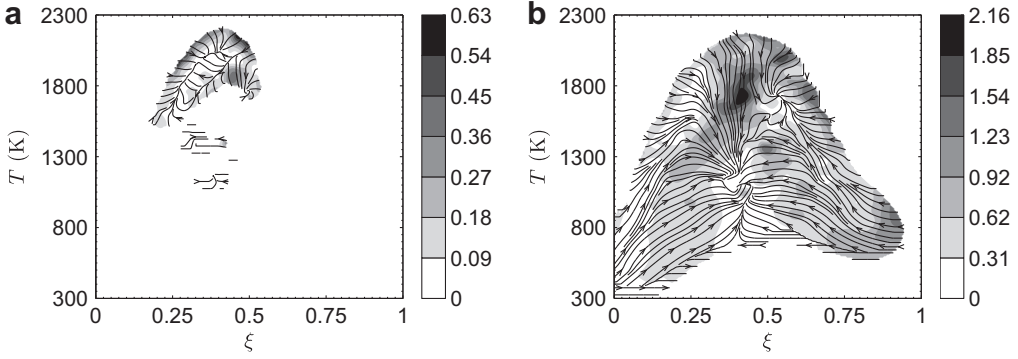
Fig. 4. The scalar diffusion and temperature diffusion filtered conditionally on both the mixture fraction and temperature for $\Delta = 3.0$ mm and $\langle \xi \rangle_L = \xi_s$ at $x/D = 30$ in flame D. (a) $\langle \xi''^2 \rangle_L = 0.0019$; (b) $\langle \xi''^2 \rangle_L = 0.059$.

perpendicular to the ridgeline. They then move along the manifold towards a stagnation point near $\xi \approx 0.4$ and $T = 2000$ K. The velocity magnitude decreases as it approaches the ridgeline. The ridgeline, therefore, appears to be a one-dimensional manifold in a two-dimensional scalar space, to which the streamlines first approach. After approaching the ridgeline the diffusion becomes one-dimensional in scalar space. The magnitude of the diffusion velocity decreases upon approaching the manifold; therefore, the diffusion towards the manifold is a fast process whereas diffusion along the manifold is a slow process.

This streamline pattern has some similarity to non-reactive scalar mixing in that the temperature is diffused towards its local mean. It can be understood in terms of the SGS mixture fraction structure for small SGS variance and the resulting quasi-equilibrium distributed reaction zones (QEDR) proposed by Bilger [14]. Because the SGS mixture fraction is well mixed, diffusion of the SGS mixture fraction is towards its local mean. With the dissipation-scale mixture fraction fluctuations smaller than the reaction zone width [8], the well-mixed SGS mixture fraction results in QEDR. In such reaction zones the temperature depends on the mixture fraction and the (local) scalar dissipation rate. This situation is different from flamelets, in which the temperature depends on the mixture fraction and the scalar dissipation rate at the stoichiometric mixture fraction. Assuming unity Lewis number, the temperature diffusion in a QEDR, therefore, depends on these fields as:

$$\frac{1}{\rho} \frac{\partial}{\partial x_i} \left(\rho D \frac{\partial T}{\partial x_i} \right)$$

$$= \frac{\partial^2 T}{\partial \xi^2} \chi + \frac{1}{\rho} \frac{\partial T}{\partial \xi} \frac{\partial}{\partial x_i} \left(\rho D \frac{\partial \xi}{\partial x_i} \right) + 2 \frac{\partial^2 T}{\partial \xi \partial \chi} D \frac{\partial \xi}{\partial x_i} \frac{\partial \chi}{\partial x_i}$$

$$+ \frac{\partial^2 T}{\partial \chi^2} \chi_\chi + \frac{1}{\rho} \frac{\partial T}{\partial \chi} \frac{\partial}{\partial x_i} \left(\rho D \frac{\partial \chi}{\partial x_i} \right), \quad (3)$$

where $\chi = D \frac{\partial \xi}{\partial x_i} \frac{\partial \xi}{\partial x_i}$ and $\chi_\chi = D \frac{\partial \chi}{\partial x_i} \frac{\partial \chi}{\partial x_i}$ are the scalar dissipation rate and the dissipation rate of χ, respectively. In a QEDR, which is not far from equilibrium, the first term is always negative, with the magnitude diminishing towards the equilibrium temperature. This trend is inconsistent with the sign change in the temperature diffusion shown in Fig. 1. The second term is close to zero near the local average mixture fraction, $\langle \xi \rangle_L$, because the scalar diffusion is small. The third term is more complex but may be small due to the mixed dissipation rate. The sign of the fourth term is determined by $\partial^2 T / \partial \chi^2$, which is chemistry dependent. For the simple chemistry model used by Bilger [14], the perturbation of a progress variable from its equilibrium value is given as $\sim -\chi^{1/2}$. If we assume $T - T_e \sim -\chi^{1/n}$, then $\partial^2 T / \partial \chi^2$ is positive, where T_e is the equilibrium temperature, and $n > 1$, reflecting a non-linear reaction rate. While χ_χ may increase when χ increases (T decreases), $\partial^2 T / \partial \chi^2$ decreases. Thus, the fourth term also is likely to be inconsistent with the trend in Fig. 1. In the last term, $\partial T / \partial \chi$ is negative. Our previous study [4] shows that the dissipation rate diffusion term in a well-mixed scalar field is similar to the mixture fraction dissipation, being generally negative for $\chi > \chi_L$ and positive for $\chi < \chi_L$, where χ_L is the local average of χ. The contribution of the last term to the temperature diffusion, therefore, is negative for temperatures above the local mean where $\chi < \chi_L$, and is positive for temperatures below the local mean where $\chi > \chi_L$, resulting in convergence of the streamlines to a manifold. Thus, it appears that only this term is consistent with the observed streamline pattern. Physically, since the temperature field in a QEDR is closely related to the scalar dissipation rate (in addition to the mixture fraction), the temperature diffusion is controlled partly by the diffusion of the scalar dissipation rate.

The observed diffusion velocity streamline pattern has some similarities to three-scalar mixing in
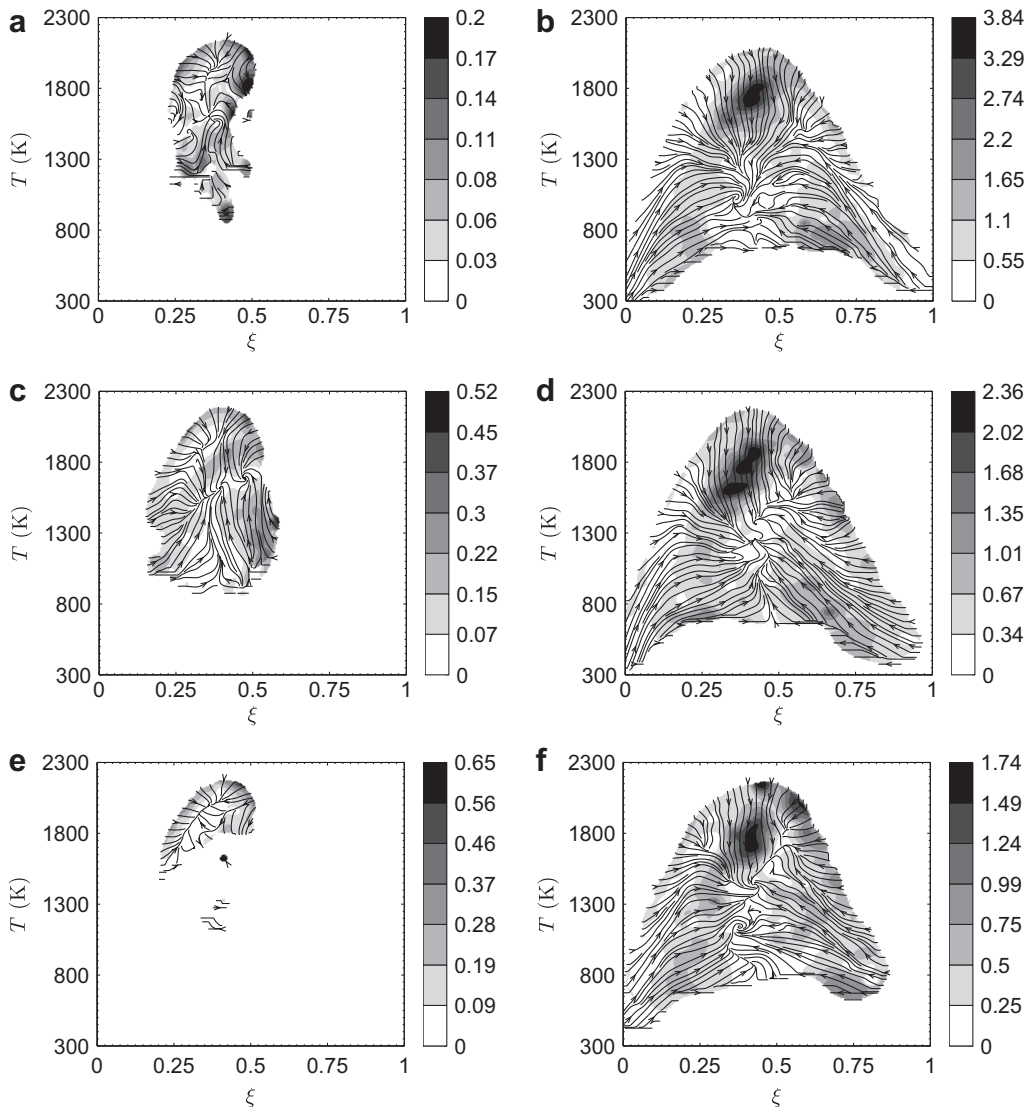
Fig. 5. The scalar diffusion and temperature diffusion filtered conditionally on both the mixture fraction and temperature for $\Delta = 3.0$ mm and $\langle\xi\rangle_L = \xi_s$ in flame E. (a), (c), and (e): $x/D = 7.5$, 15 and 30, respectively. Small SGS variance ($\langle\xi''^2\rangle_L = 0.0011$, 0.0028, and 0.0018); (b), (d), and (f): the same locations. Large SGS variance ($\langle\xi''^2\rangle_L = 0.081$, 0.064, and 0.044).

a non-reacting flow. In our recent study of three-scalar mixing in a co-axial jet, which will be published in a separate paper, the three scalars are introduced by a center jet, an annular flow, and co-flow air, with the second scalar initially separating the first and the third. The resulting diffusion velocity streamline pattern in this jet is qualitatively similar to that in Fig. 1a. There is a manifold to which the streamlines converge quickly. They then move at a slower velocity on the manifold. During the convergence the diffusion of the second scalar is faster than the first, analogous to the fast diffusion of temperature

shown in Fig. 1a. In this jet the three scalars have a similar spatial relationship to that among the mixture fraction, the temperature, and the co-flow air in a non-premixed flame; therefore, the temperature in the QEDR has a similar physical-space structure as the annulus flow, separating the other two scalars. Such a structure is different from three scalar mixing cases where the three scalars are arranged symmetrically in physical space [15]. Nevertheless, the mixing of temperature in the QEDR is controlled by very different processes (the chemistry and the diffusion of the scalar dissipation rate).

For large SGS variance (Fig. 1b) the streamlines for very rich ($\xi > 0.6$) and lean ($\xi < 0.2$) mixtures generally move in the direction of the ridgeline of the FMDF (see Ref. [9]) towards the stoichiometric mixture fraction. Our previous results have shown that for large SGS variance the SGS flames are strained flamelets. Here the mixture fraction profiles have approximately error-function profiles (ramp-cliff structure). Thus, the diffusion of the mixture fraction is towards the center of the profiles (appears to be near $\xi = 0.45$). For very rich and lean mixtures the temperature depends approximately linearly on the mixture fraction; therefore, its diffusion is proportional to the mixture fraction diffusion, resulting in straight diffusion streamlines along the ridgeline.

Near the peak temperature the mixture fraction diffusion is small because this region is close to the center of the error-function profiles where the curvature of the profiles is zero. The temperature diffusion is negative due to the negative curvature of the temperature profiles as a function of the mixture fraction and the approximately linear mixture fraction profiles. Consequently, the streamlines starting from the equilibrium curve near $\xi = 0.45$ move nearly vertically towards lower temperatures. As the streamlines move towards lower temperatures, the scalar dissipation rate increases, corresponding to more strongly strained flamelets with stronger diffusion. The largest magnitude of the diffusion velocity vector occurs for temperatures near 1600–1800 K. Below this temperature range the temperature profiles become broader in the mixture fraction space with smaller curvatures, resulting in lower temperature diffusion. There appears to be a stagnation point at $\xi \approx 0.4$ and $T = 1300$ K. Note that although this point appears to be the "center" of diffusion, it does not correspond to the conditional mean temperature for this mixture fraction value.

The streamlines starting from the very rich and lean regions move up along the ridgeline and turn near $\xi \approx 0.27$ and $T = 1600$ K and near $\xi \approx 0.55$ and $T = 1600$ K, respectively, towards the stagnation point. The temperature diffusion changes sign near these points, where the inflection points of the temperature profiles are located. This result is consistent with our previous study [9] which shows that the temperature dissipation rate is largest in this region. Below these points the diffusion is dominated by mixing whereas above it the diffusion is strongly influenced by both mixing and reaction. This streamline pattern is also consistent with the structure of flamelets.

Figure 1b also shows that in the very rich and lean regions the streamlines generally first approach the FMDF ridgeline and then move along it. One possible reason for this trend is the diffusion among flamelets in the direction along the iso-mixture fraction surfaces. Because the ridgeline represents the flamelets with the highest probability of occurrence, the flamelets nearby tend to diffuse towards the ridgeline. Another possibility is that in the SGS fields with large SGS variance, in addition to the ramp-cliff structure, there are also "background" mixture fluctuations, which are generally well mixed and tend to have smaller dissipation time scales, causing diffusion streamlines to converge to those of the flamelets. There also appears to be two diffusion processes involved: in the fast process the streamlines approach a one-dimensional manifold and the in the slow process they move along the manifold.

At $x/D = 15$ the results for small SGS variance (Fig. 2a) are similar to those at $x/D = 7.5$ for the samples with temperatures higher than 1900 K, where the mixing of temperature is dependent on the mixture fraction, the scalar dissipation rate, and the chemistry. There is, however, a second manifold with a stagnation point near $\xi = 0.4$ and $T = 1600$ K, probably due to the mixing between the burning and extinguished samples, which have temperatures as low as 1000 K. The mixing process at these temperatures is different from that at higher temperatures. Here the reaction rate has decreased significantly due to local extinction. The temperature no longer strongly depends on the scalar dissipation rate and the chemistry. Its mixing (e.g., Ref. [16]), therefore, becomes similar to that of a non-reactive scalar. In addition, because the SGS mixture fraction is well mixed, the mixing process is similar to three-scalar mixing in a homogeneous scalar field. The fast convergence to the manifold in the direction of temperature suggests that the mixing of temperature is faster than that of mixture fraction.

To understand this streamline pattern further, we compute the conditionally filtered diffusion with the Favre filtered temperature as a third conditioning variable, in addition to the Favre filtered mixture fraction and the Favre SGS scalar variance. The samples used to obtain Fig. 2a are separated into two groups, one with $\langle T \rangle_L > 1800$ K and the other with $\langle T \rangle_L < 1800$ K. The streamline pattern for the former (Fig. 3a) is similar to that at $x/D = 7.5$. There is one manifold, to which the streamlines converge. The streamlines for the latter (Fig. 3b) converge to approximately 1600 K, corresponding to the second stagnation point in Fig. 2a. The diffusion vector pattern shown in Fig. 2a, therefore, can be viewed as a superposition of two different states of the SGS flames: mixing in nearly fully burning distributed reaction zones and mixing between fully burning and extinguished distributed reaction zones. Between the stagnation point near $\xi = 0.4$ and $T = 1600$ K and the one near 2000 K, there appears to be a saddle point (or a saddle line) separating the two regions. The location of the saddle point probably depends on the relative strength of the two stagnation points.

For large SGS variance (Fig. 2b) the overall diffusion pattern for burning samples are similar to that at $x/D = 7.5$. For the lean mixtures the streamlines turn towards the stagnation point as early as $\xi \approx 0.15$ and $T = 1300$ K. There are more extinguished samples, for which the streamlines move primarily in the direction of mixture fraction towards $\xi \approx 0.4$, with only modest increases in temperature. These trends indicate that for these samples the mixture fraction diffusion is initially much faster than the temperature diffusion. An examination of the instantaneous profiles in the scalar space shows straight lines running from the lean side to the rich side, largely in the same direction of the diffusion vectors; therefore, these lines are extinguished flamelets, hence the smaller temperature diffusion. For these extinguished flamelets, temperature diffusion can occur in the direction of the mixture fraction gradient as well as along the iso-mixture fraction surface. The latter is diffusion among burning and extinguished flamelets (flamelet–flamelet interaction). Near $\xi = 0.4$ the scalar is close to the center of the error-function profiles (ramp-cliff structure) where mixture fraction diffusion is zero; therefore, the streamlines move largely in the direction of temperature.

For rich samples there are a significant number of nearly straight streamlines running from very rich region ($\xi \approx 0.9$, $T \approx 500$ K) towards the region corresponding to the pilot. These streamlines may be due to the pilot flame separating the rich and lean mixtures, and are essentially a result of mixing between the pilot and the fuel/air streams without reactions. The pilot flame, therefore, appears to have some influence on the diffusion. Our previous results [9] have shown that it also has some influence on the temperature dissipation. These streamlines turn near $\xi = 0.5$ and $T = 1600$ K towards the stagnation point, a result of the strained flamelets. Similar to the results at $x/D = 7.5$, the rich samples close to equilibrium diffuse first towards a manifold (the ridgeline of the FMDF) and then follow the manifold. The approach to the manifold is faster than at $x/D = 7.5$. In the low temperature region the temperature diffusion is faster than for the lean samples.

At $x/D = 30$ the results for small SGS variance (Fig. 4a) are similar to those at $x/D = 15$. For large SGS variance (Fig. 4b) the influence of the pilot is much less evident with the streamlines from the rich side with temperature below 1200 K moving in a direction much closer to the horizontal direction toward $\xi \approx 0.4$, indicating that the SGS mixing has progressed much further and that there is little pure pilot gas left. These streamlines are a result of mixing along scalar profiles running from the rich to the lean side (extinguished flamelets). Note that at $x/D = 15$ the streamlines in this region are closer to the direc-

tion of the mixing line between the pilot and the fuel stream, suggesting that the influence of the pilot on the diffusion is stronger than the effects of the extinguished flamelets.

The results for flame E (Fig. 5) are qualitatively similar to those for flame D. Due to the higher Reynolds number, flame E already has a significant amount of local extinction at $x/D = 7.5$, with the largest amount occurring at $x/D = 15$. For small SGS variance, the temperature decreases to as low as 1000 K at $x/D = 7.5$ and $x/D = 15$. The amount of local extinction is also much larger than in flame D. The diffusion streamlines at $x/D = 15$ is similar to those for flame D. But the lower stagnation point occurs at a slightly lower temperature. In addition, the stagnation point near 2000 K appears to be weaker, which may be due to the stronger stagnation point near 1600 K resulting from the larger amount of local extinction.

For large SGS variance, the streamline patterns also are generally similar to those for flame D. At $x/D = 7.5$ the streamlines for the extinguished samples are approximately symmetric with respect to $\xi = 0.4$. These streamlines become asymmetric at $x/D = 15$, again perhaps due to the influence of the pilot flame. They become more symmetric at $x/D = 30$.

The results for the diffusion streamlines in Figs. 1a and 2a suggest that the SGS mixing processes for small SGS variance can be modeled in a way similar to non-reactive scalars. For QEDRs, which have temperatures not far from the equilibrium values, the mixing can be modeled through the mixing of mixture fraction and the scalar dissipation rate, due to the strong influence of the latter on the temperature. The similarities of the streamline pattern to those of three-scalar mixing in a co-axial jet suggest that the mixing process needs to be modeled in a way that reflects the separation of two of the scalars (the mixture fraction and the co-flow) by the third (the scalar dissipation rate) in physics. For SGS fields with lower temperature (e.g., $\langle T \rangle_L < 1800$ K), the SGS mixing can be modeled as the mixing of mixture fraction and the non-reactive temperature due to the decoupling of temperature from the chemistry and the scalar dissipation rate as a result of much reduced reaction rate. In contrast to the mixing in QEDRs, the mixing process for these SGS fields resembles three-scalar mixing in a homogeneous scalar field, and therefore can be modeled as such. For large SGS variance, mixing models need to incorporate the physics of the more complex diffusion velocity pattern resulting from the flamelet structure and local extinction.

In the present study the mixture fraction is calculated using Bilger's definition, which maintains the stoichiometric mixture fraction in the presence of differential diffusion. In the Sandia flames the diffusivities for ξ and T are very close, therefore, we expect the differential diffusion effects on the

conditionally filtered diffusion of these two variables to be weak. For the conditionally filtered diffusion of spectis mass fractions the effects may be stronger due to the wide range of diffusivities. On the other hand, differential diffusion effects are weaker (at least in the average sense) in turbulent flames than in laminar flames. It is unclear at this time how strong they will be for the species mass fraction diffusion.

4. Conclusions

In the present work we used data obtained in turbulent partially premixed flames (Sandia flames D and E) to study the influence of the SGS mixture fraction structure on the diffusion of the mixture fraction and temperature. The Favre filtered mixture fraction and the Favre SGS scalar variance were used as conditioning variables for analyzing the scalar filtered mass density function and other SGS variables. The main findings are:

- For small SGS scalar variance, at high temperature (the burning samples) the conditionally filtered diffusion of the mixture fraction and temperature, represented by streamlines, generally move towards the ridgeline of the FMDF and then move along it. There are, therefore, two mixing process, one fast and one slow. The mixing of temperature is controlled by the scalar dissipation rate and the chemistry.
- Mixing between burning and extinguished samples generally causes the streamlines to converge to an intermediate temperature of approximately 1600 K. The mixing of temperature is more similar to that of a non-reactive scalar.
- For large SGS scalar variance, the mixing processes are more complex. Part of the streamline pattern is consistent with flamelets. The streamlines for very rich and lean mixtures generally converge towards the ridgeline of the FMDF and move upward along it, again indicating two mixing precesses, one fast and one slow.
- Low temperature samples are largely extinguished flamelets, which cause the streamlines to move in straight lines predominately in the direction of the mixture fraction towards $\xi = 0.4$, approximately the center of the ramp-cliff structure.
- At $x/D = 15$ the mixing of the pilot flame and the fuel stream also appear have some impact on the streamline pattern, resulting in nearly straight streamlines connecting the fuel and the pilot in the scalar space, indicating that the dissipation rate is large and that there is essentially no reaction in this region.

The present study shows that the mixing regimes and the resulting streamline patterns for the conditionally filtered diffusion are important SGS mixing characteristics of the flames. These patterns are challenging tests for mixing models.

References

[1] S.B. Pope, *Computations of Turbulent Combustion: Progress and Challenges*, Proc. Combust. Inst. 23 (1990) 591.
[2] P.J. Colucci, F.A. Jaberi, P. Givi, S.B. Pope, *Filtered density function for large eddy simulation of turbulent reacting flows*, Phys. Fluids 10 (1998) 499.
[3] C. Tong, *Measurements of conserved scalar filtered density function in a turbulent jet*, Phys. Fluids 13 (2001) 2923.
[4] A.G. Rajagopalan, C. Tong, *Experimental investigation of scalar–scalar-dissipation filtered joint density function and its transport equation*, Phys. Fluids 15 (2003) 227.
[5] D. Wang, C. Tong, *Conditionally filtered scalar dissipation, scalar diffusion, and velocity in a turbulent jet*, Phys. Fluids 14 (2002) 2170.
[6] D. Wang, C. Tong, S.B. Pope, *Experimental study of velocity filtered joint density function and its transport equation*, Phys. Fluids 16 (2004) 3599.
[7] D. Wang, C. Tong, *Experimental study of velocity-scalar filtered joint density function for les of turbulent combustion*, Proc. Combust. Inst. 30 (2005) 567.
[8] D. Wang, C. Tong, R.S. Barlow, A.N. Karpetis, *Experimental study of scalar filtered mass density function in turbulent partially premixed flames*, Proc. Combust. Inst. 31 (2007) 1533.
[9] J. Cai, D. Wang, C. Tong, R.S. Barlow, A.N. Karpetis, *Investigation of subgrid-scale mixing of mixture fraction and temperature in turbulent partially premixed flames*, Proc. Combust. Inst. 32 (2009) 1517.
[10] A.N. Karpetis, R.S. Barlow, *Measurements of flame orientation and scalar dissipation in turbulent partially premixed methane flames*, Proc. Combust. Inst. 30 (2005) 665.
[11] R.S. Barlow, A.N. Karpetis, *Measurements of scalar variance, scalar dissipation, and length scales in turbulent piloted methane/air jet flames*, Flow Turb. Combust. 72 (2004) 427.
[12] C. Tong, J.C. Wyngaard, S. Khanna, J.G. Brasseur, *Resolvable- and subgrid-scale measurement in the*

atmospheric surface layer: technique and issues, *J. Atmos. Sci.* 55 (1998) 3114.

[13] G. Wang, A.N. Karpetis, R.S. Barlow, *Dissipation length scales in turbulent nonpremixed jet flames*, *Combust. Flame* 148 (2007) 62.

[14] R.W. Bilger, *The Structure of Turbulent Nonpremixed Flames*, *Proc. Combust. Inst.* 22 (1988) 475.

[15] A. Juneja, S.B. Pope, *A DNS study of turbulent mixing of two passive scalars*, *Phys. Fluids* 8 (1996) 2161.

[16] P. Sripakagorn, S. Mitarai, G. Kosaly, H. Pitsch, *Extinction and reignition in a diffusion flame: a direct numerical simulation study*, *J. Fluid Mech.* 518 (2004) 231.